Ultrasound in Med. & Biol., Vol. 27, No. 11, pp. 1451–1460, 2001

0301-5629/01/$–see front matter

PII: S0301-5629(01)00453-7

● *Original Contribution*

NONINVASIVE ASSESSMENT OF VOCAL FOLD MUCOSAL WAVE VELOCITY USING COLOR DOPPLER IMAGING

YIO-WHA SHAU,* CHUNG-LI WANG,† FON-JOU HSIEH† and TZU-YU HSIAO‡

*Institute of Applied Mechanics, National Taiwan University, Taipei, Taiwan; †Department of Diagnostic Ultrasound and ‡Department of Otolaryngology, National Taiwan University Hospital, Taipei, Taiwan

(*Received* 3 *May* 2001; *in final form* 31 *July* 2001)

Abstract—The vibratory movement of the vocal folds (VF) plays an important role in normal function of phonation. We developed a noninvasive technique to quantify the human mucosal wave velocity (MWV) *in vivo* using color Doppler imaging (CDI). During phonation, the motion of mucosa-air interface generates a unique pattern of US color artefacts that assist the identification of true VF location. An *in vitro* study using a vibrating string phantom was conducted to investigate how the CDI displayed a vibrating soft tissue at high frequency. The vibrating amplitude, frequency, mass density and the acoustic impedance of the soft tissues were found to dominate the formation of color artefacts. Based on the model of finite string with fixed ends, we estimated the mean MWV for 10 adult volunteers (6 men, 4 women, ages 34 ± 5 years) with normal VF function. The mean MWVs for the men were found to vary from 2.1 to 10 m/s in a frequency range of 85 to 310 Hz at their comfortable pitch and intensity, and the women typically had higher MWVs that varied from 5.0 to 16.5 m/s in a frequency range of 180 to 480 Hz. The MWV increased linearly with the frequency and there was no observable difference in mucosa stiffness due to the effect of gender. The variation in MWV as it propagates vertically can be seen from the color and shape of the artefacts. The VF polyp resulted in abnormal MWV and different CDI vibratory artefacts. The CDI artefacts provide insight on the dynamics of mucosa structure during phonation, and the method presented is promising for noninvasive monitoring of laryngeal functions clinically. (E-mail: tzuyu@ha.mc.ntu.edu.tw) © 2001 World Federation for Ultrasound in Medicine & Biology.

Key Words: **Color Doppler image, Vocal fold, Mucosal wave velocity, Phonation function, Ultrasound artefacts, Laryngeal ultrasonography.**

INTRODUCTION

Although clinical ultrasound (US) has been widely used in various noninvasive musculoskelatal diagnoses, its application on the laryngeal examination has been limited due to the spatial resolution and the dynamic response to tiny high-frequency movements (Baken and Orlinkoff 2000). The three-dimensional (3-D) vibratory movements of the vocal folds (VF) are essential for voice production. Among the basic functions of the human larynx, the phonation performance is the most complex and the least well understood activity (Sasaki and Weaver 1997). Therefore, sophisticated noninvasive technologies that combine photoglottography (PGG), electroglottography (EGG) or video laryngostroboscopy with aerodynamic theories have been developed to investigate the laryngeal function and the neurophysiology of phonation (Hirano 1981; Hanson et al. 1995; Lin et al. 1999). To visualize the laryngeal activity *in vivo* under normal articular movements, fiberoptics were inserted into the lower pharynx *via* the nasal cavity (Sawashima 1977). The ultrasonography of the larynx would provide further details of the VF cartilaginous and endolaryngeal structures. Unfortunately, the works were successful only in infants and children (Garel et al. 1990; Friedman 1997), and the B-mode US images for adult true VF and vocal muscles, which appear as hypoechoic structures, were often inconclusive (Raghavendra et al. 1987). Nevertheless, vocal cord paralysis that alters the symmetry of VF vibrations can be easily identified using echoglottography (Schindler et al. 1990; Ooi et al. 1995; Friedman 1997).

Hirano (1974) proposed a body-cover mechanical model to simulate multilayered VF structures (Fig. 1), in which two upper and lower masses of the "cover" (representing the epithelium and the superficial layer of the

Address correspondence to: Tzu-Yu Hsiao, M.D., Ph.D., Associate Professor, Department of Otolaryngology, National Taiwan University Hospital, 7, Chung-Sun South Road, Taipei 10016 Taiwan. E-mail: tzuyu@ha.mc.ntu.edu.tw

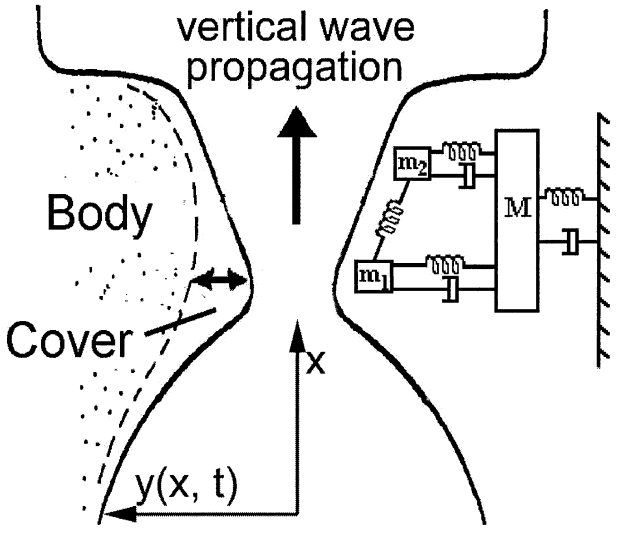

Fig. 1. Coronal view of the vocal folds showing Hirano's body-cover theory (left) and the corresponding masses-springs model (right). The mucosal bulge moves horizontally and the mucosal wave propagates vertically.

lamina propria) that interconnected with a spring were coupled laterally to the "body" mass (the vocal muscle and ligament) by springs and viscous dampers (Ishizaka and Matsudaira 1972). Because the cover is the main vibratory element of the VF, the mechanical properties of the mucosa and the aerodynamic forces acting on the VF play important roles in the formation of voice.

Direct measurement of the stiffness of human VF during normal phonation is extremely difficult because the measurement devices or markers must be in contact with the VF (Isshiki et al. 1985; Berke 1992; Berke and Smith 1992; Tran et al. 1993). However, for an elastic medium, the wave propagation velocity (c) is directly correlated with the intrinsic tension force (T) and inversely proportional to its mass length-density (μ) (Achenbach 1984; Fetter and Walecka 1980).

$$c = \sqrt{\frac{T}{\mu}} \tag{1}$$

For a given tissue displacement, the tension (T) is proportional to the stiffness or elastic modulus of the medium. This provides an alternative way of estimating soft tissue stiffness noninvasively. Both extrinsic longitudinal tension of the VF cover and the internal stiffening of the VF body would contribute to the change in overall VF stiffness. Due to the sinusoidal nature of the mucosal wave, the VF displacement, $y(x, t)$, can be approximated by (Nasri et al. 1994):

$$y(x, t) = A_o \cos[2\pi(x - ct)/\lambda], \tag{2}$$

where A_o is the maximum amplitude of the horizontal displacement (Fig. 1), c is the mucosal wave velocity (MWV) traveling vertically, and λ is the wavelength. The horizontal displacement velocity (HDV) can be derived from the time rate of change of mucosal geometry, $\partial y(x, t)/\partial t$:

$$v = \partial y(x, t)/\partial t = 2\pi A_o(c/\lambda) \sin[2\pi(x - ct)/\lambda]. \tag{3}$$

Apparently, the magnitude of the HDV (v) of the VF is linearly proportional to the MWV (c). The HDV that determined from the displacement of the upper edge of the VF can be measured optically without touching the VF. Therefore, recent laryngeal researches for the mechanical properties of the VF have been focused on the measurements of mucosal wave propagation in canine or human larynges (Tanaka and Hirano 1990; Sloan et al. 1993; Titze et al. 1993; Nasri et al. 1994; Hanson et al. 1995).

The VF that vibrates typically at a fundamental frequency (F0) up to a few hundred hertz poses a great challenge to the US imaging system. However, the US causes the least interference to the VF during normal phonation; it will be the most promising *in vivo* tool for routine laryngeal examination if the interpretation of VF characteristics can be improved quantitatively. In our preliminary US study of the VF functions, we measured the HDV of the VF cover using color Doppler imaging (CDI) and correlated it with the stiffness of the mucosa (Hsiao et al. 2001). The aim of this study was to develop a novel technique that can quantify the human MWV directly and noninvasively using a commercially available color duplex US system. Based on the fundamental physics of a travelling wave, the wave velocity is simply the product of frequency and wavelength ($c = f\lambda$). The phonation frequency, F0, can be measured easily with a microphone and a spectrum analyzer, and the MVW (c) can be found if one can resolve the wavelength (λ) for the vertical movement of the VF cover. Therefore, our study was focused on how the CDI visualized the vibratory movements of soft tissues and how to use the CDI artefact to measure the mucosal traveling wave. Both *in vitro* phantom validation and *in vivo* VF measurements using CDI have been performed to demonstrate the current methodology.

MATERIALS AND METHODS

The study was performed with a commercially available, high-resolution US scanner (HDI-5000, ATL, Bothell, WA) with a 5- to 12-MHz linear array transducer (L12 to 5 38 mm, ATL). The CDI frame rate (f_s) of the US system, which is typically of a few hertz, is much too slow to capture the movement of the VF in real-time.

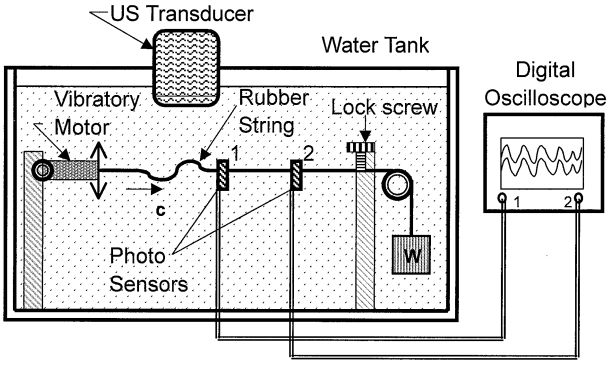

Fig. 2. Setup and instrumentation for the *in vitro* measurement of TWV for a vibrating string. A vibrating motor drives the motion of the rubber string on the left at the frequency range of 50 to 235 Hz. The TWV (c) traveling toward the right was measured from the delay of the interrupt signals between two photosensors with fixed spacing of 2 to 3 cm. The tension of the string can be adjusted by the weight (W).

The CDI of VF exhibited strobe motion artefacts that were generated by the vibratory movements of the VF cover–air interface, and the artefact patterns changed systemically with the intensity and frequency of the voice.

In vitro study of vibrating string

To understand the driving mechanism of CDI artefacts and to make a quantitative measurement of the MWV, a phantom was built to simulate the VF with a prescribed vibrating frequency (f) and with a known traveling wave velocity (TWV). The phantom consisted of a vibrating motor capable of delivering vibrating frequencies ranging from 50 to 235 Hz under voltage supply of 1.2 to 4.5 V and a rubber string of mass length density (μ) of about 0.026 g/cm (Fig. 2). The tension of the string (T) was adjusted by changing the weight (W) that connected to the string *via* a pulley. With one end connected to the vibrating motor, the other end of the string was secured with a locking screw. The cross-sectional area of the rubber string is about 2.25 mm^2 and the length (L) can be varied from 2 cm to 15 cm. In some cases, we added additional mass on the string to simulate a VF polyp or stiffened spots and then observed the differences in CDI.

The vibrating string was immersed in a water container at about 6 to 7 cm above the bottom surface to reduce the interference of US reflection, and the US transducer was placed at about 2 to 3 cm above the string. Furthermore, to see the effects of CDI frame rate on the color artefact, we selected different CDI line-density settings that allowed us to visualize the string vibration at the frame rates (f_s) with the range from 5 to 7 Hz.

The TWV (c) was measured by using a pair of low-cost U-shaped slotted photograph interrupters (PTIR-902, Team House Ltd., Taipei, Taiwan) that consisted of a light-emitting diode (LED) and a phototransistor. The string was positioned to obstruct the light of the LED and cast a shadow on the surface of the phototransistor. Within a range of about 1.5 mm displacement, the output voltage of the phototransistor varied from 0 to 3 V and was linearly proportional to the position of the string. Therefore, no instrumental amplifier was needed. During the vibratory movement of the string, the sinusoidal output signals of the two optical sensors were monitored simultaneously on a four-channel digital oscilloscope (TDS-224, Tektronix, Wilsonville, OR). The TWV (c) was calculated based on the separation distance (Δx) of the two optical sensors and the time delay (Δt) of the traveling wave. The photograph sensor used in this study was capable of measuring a displacement of 10 μm at a time resolution of 10 μs.

Because the phantom was designed to simulate the VF vibration and to study the physical mechanism of CDI artefacts, two types of driving forces were applied to the vibrating string. 1. Phantom mode A: string vibration generated by a vibrating motor with variable amplitudes on one end. Because the tension of the string was proportional to the motor power that increased with the vibrating frequency, the TWV (c) also increased with the frequency. 2. Phantom mode B: string vibration generated by a vibrating motor with fixed amplitude on one end. In this case, the string was constrained to move up and down with constant amplitude of about 2 mm at a length of $L = 12$ cm. Therefore, the tension of the string and the TWV (c) were kept constant at various vibrating frequencies.

In vivo study

A total of 10 healthy adult volunteers (6 men and 4 women) aged 34 $\pm$ 5 years with normal VF function were recruited for this study. Each gave informed consent to take part in the experiments. Ultrasound examination was performed with the subjects in sitting position (Fig. 3). Movements of the VF were monitored in prolonged phonation of various pitches. The voice signal was detected with a precision microphone (ECM-672, SONY, Tokyo, Japan) and the F0 was measured and displayed on the digital oscilloscope (TDS-224) that was equipped with a fast Fourier transform (FFT) module (TDS2 MM). To verify the difference in F0s given by the voice and the VF, an accelerometer (AS-50B, Kyowa, Tokyo, Japan) in some cases was simultaneously attached to the larynx to measure the VF vibration directly.

The sound level of the voice was measured with a precision sound level meter (Type 2235, Brüel & Kjær, Nærum, Denmark) that was placed in front of the subject

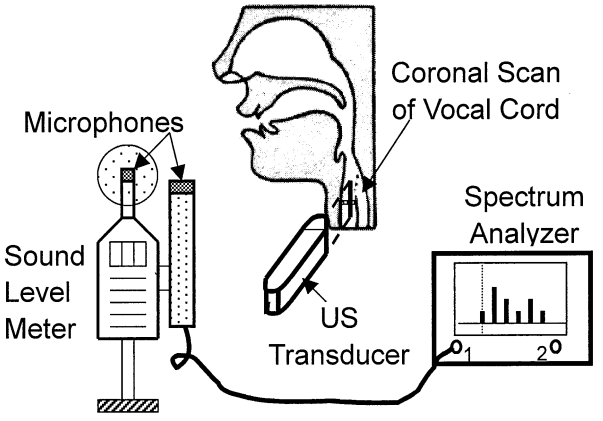

Fig. 3. Setup and instrumentation for the *in vivo* measurement of human VF MWV. Subjects in sitting position were asked to utter a voice at their comfortable pitch and SPL. US transducer was placed on the anterior of the larynx to give the coronal view of the VF. Microphones were used to monitor the SPL and the fundamental frequency of the voice on site.

at a distance of about 30 cm away from the mouth. By using "A" frequency weighting and "random" sound incidence settings in the sound level meter, the subjects were asked to keep the sustained vowel at a sound level of about 65 to 75 dB for men and 70 to 80 dB for women.

To measure the mucosal wave propagation, a correct positioning of the US transducer is obtained if the US scanning plane gives a coronal view of the vocal cord. The US transducer was placed vertically at about anterior one fourth of the thyroid cartilage lamina (Fig. 4a), which was at the midportion of antero-posterior VF dimension where the VF vibrated at the maximal excursion (Isshiki 1989). By using color Doppler imaging, the mean velocity (HDV) of tissue displacement in the VF cover area can be measured (Fig. 4b, c). The red-blue color of the CDI artefact signifies the strobe-motion of the vibratory VF toward and away from the US transducer, respectively.

For each measurement, the VF structure was first observed with a scanning window of width of 3.8 cm and depth of up to 4 cm. The B-mode frame rate was typically about 25 Hz. For a sinusoidal VF vibration, the mean velocity toward the US transducer (CDI red code) is the same as that away from the transducer (CDI blue code). In the color mode, to obtain a better CDI velocity resolution in the higher range, the measuring velocity scale was set to the maximum (0 to 128.3 cm/s) with the baseline offset. The CDI artefact wavelength (λ_{CDI}) was given by the interval of a pair of bright-dark strips (Fig. 5a). In most of the cases, a scanning depth of 4 cm was high enough to detect the vibratory part of the VF. The corresponding pulse-repetition frequency (PRF) was 10,000 Hz, and the CDI frame rate (f_s) was about 6 Hz, typically. Two women patients who suffered from phonation disorder (unilateral VF polyp) were also included in this study.

RESULTS

Figure 6 depicts the TWV (c) measured for a rubber string (phantom mode A) that vibrates at various frequencies. The TWV of the string was linearly proportional to the vibrating frequency because a higher driving force was given. Figure 5a–d shows the results of CDI for such a string that vibrates at frequencies of f = 57, 119, 161 and 204 Hz, respectively under variable tensile forces. The vibratory movements of the string caused artefact strips underneath the string in a regular fashion. The locations where small plastic tapes were attached (arrows) generated strong artefact reflections.

The wavelengths of the artefact strips (λ_{CDI}) that were measured directly from the CDI and the corresponding TWV(c) measured by the photograph sensors are listed in Table 1. It is obvious that the CDI wavelength (λ_{CDI}) decreases with the increase in vibrating frequency (f). Moreover, the CDI frame rate (f_s) also played an important role on the generation of vibratory artefacts. Figure 7 shows that the CDI of a string vibrates at f = 57 Hz and the frame rates (f_s) were altered from 5 to 7 Hz. The strings appeared in grey-colored wavy shapes and had about the same amplitudes under different CDI frame rates (f_s), but the string wavelengths observed increased with f_s. The color artefacts under the string correlated directly with the strobe waveform of the string. Apparently, the CDI artefact wavelength (λ_{CDI}) correlated positively with the frame rate (f_s). Because the TWV (c) is known (406 cm/s), we find the ratio of true wavelength (λ) to the CDI wavelength (λ_{CDI}) can be factorized as a function of the frequency ratio, (f/f_s).

For the phantom mode B, the typical results of CDI for a string that is vibrating with fixed TWV (*i.e.*, c = 938 and 1470 cm/s) are listed in Table 2. Again, the CDI artefact wavelengths (λ_{CDI}) were found to correlate strongly with the frequency ratio (f/f_s). After the extensive tests by varying the length (L) and tension (T) of the string and taking all the parameters into account, we found that the CDI artefact wavelength (λ_{CDI}) can be factorized into a simple relationship:

$$\lambda_{CDI} \cong (3.94 \pm 0.17) \cdot (f_s/f) \qquad \text{(cm)} \qquad (4)$$

Figure 8a and b shows the typical coronal views of VF CDI for a male subject that was phonating at a F0 of 112 Hz with different sound pressure levels, SPL = 65 dB and 80 dB, respectively. Although the detailed VF structure could not be seen clearly, the mucosal waves that were traveling vertically generated an "Africa-like" color

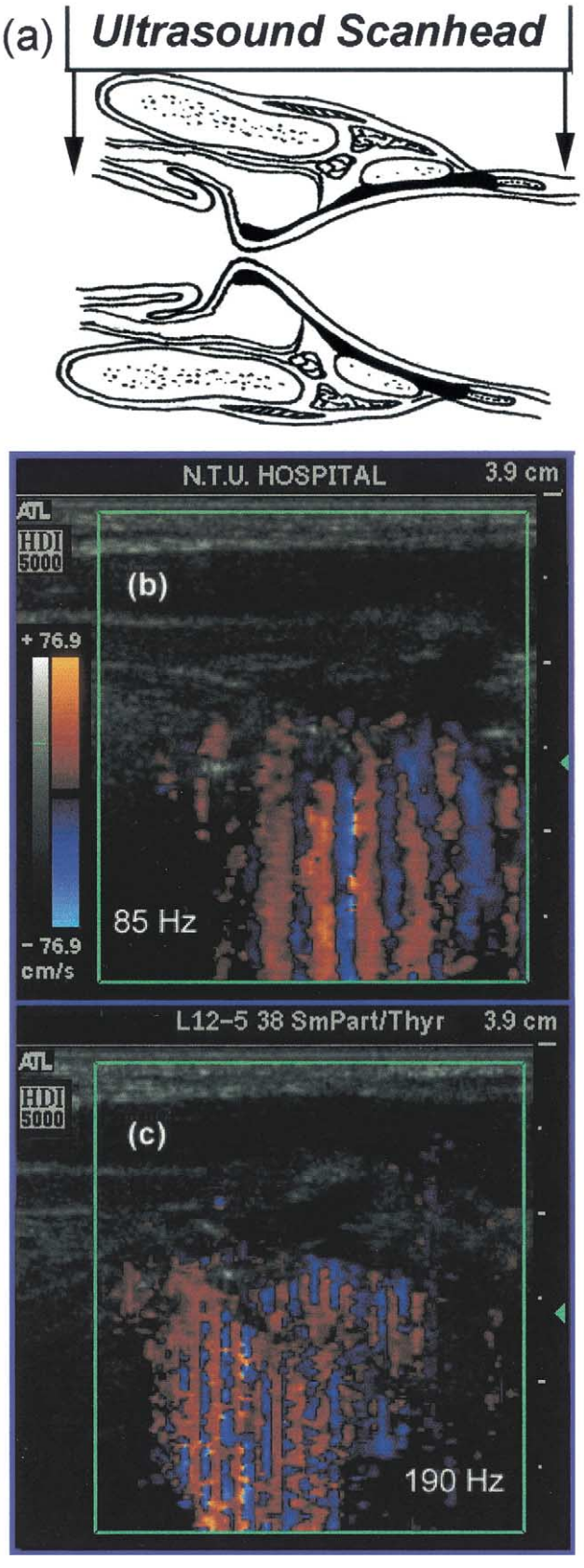

Fig. 4. (a) Schematic of US coronal scan of the VF; (b) typical CDI for the VF vibrating at frequency f = 85 Hz; (c) f = 190 Hz in coronal view.

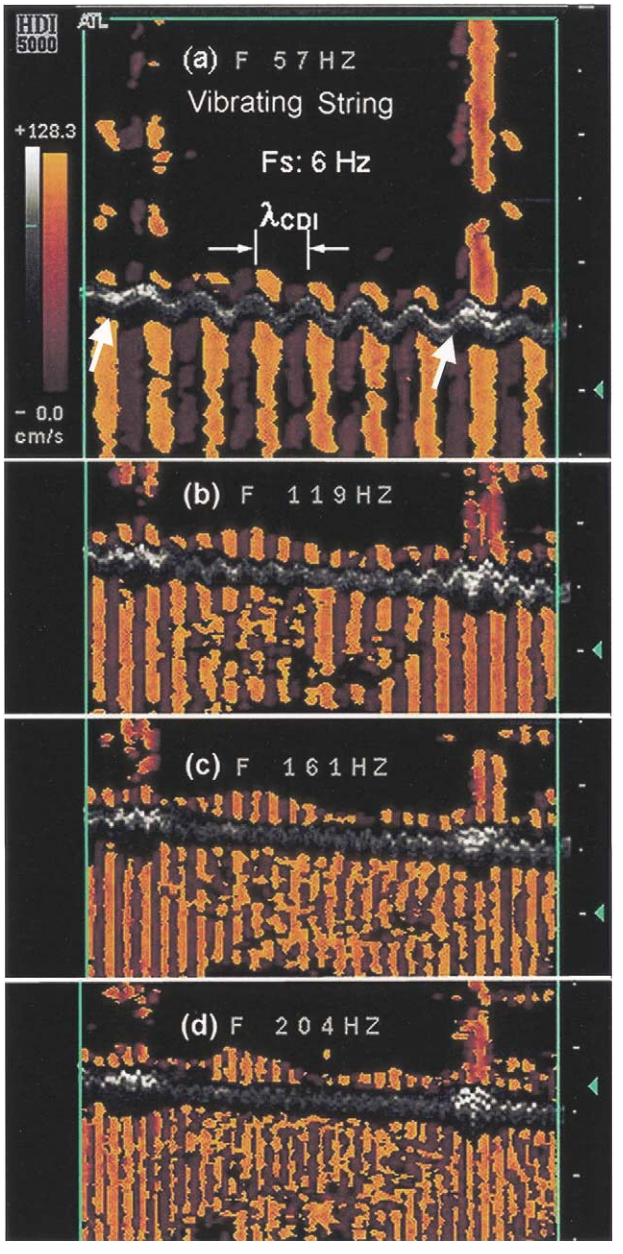

Fig. 5. Effects of vibrating frequency on the display of CDI color artefacts. (a) f = 57 Hz; (b) f = 119 Hz; (c) f = 161 Hz; (d) f = 204Hz. Two small pieces of plastic tape (arrows) were attached to the rubber string on both sides to simulate the hardened spots of the VF.

artefact underneath the VF-airspace interface. The VF "body" (vocal muscle and ligament) appeared in a grey color embedded in the CDI motion artefact. The F0 of the voice recorded by the microphone was found identi-

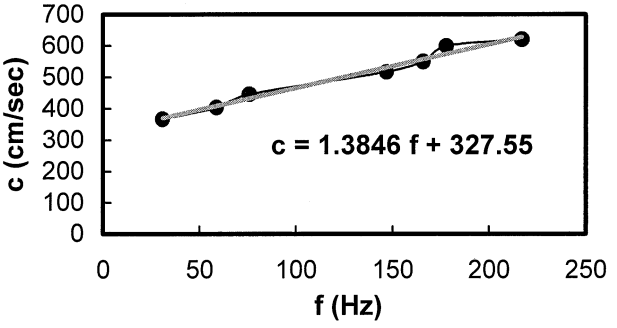

Fig. 6. Variation of TWV (c) with respect to the vibrating frequency (string phantom A) in which the motor power increases with frequency.

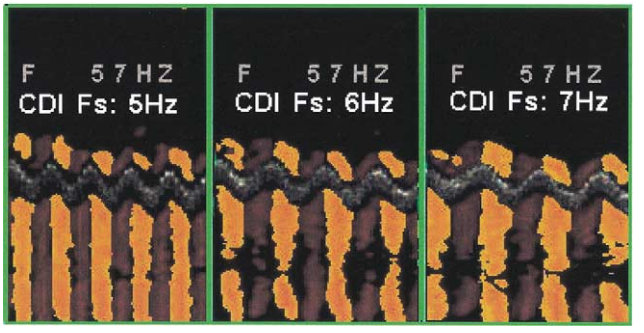

Fig. 7. Effect of CDI frame rate (fs) on display of color artefacts. fs = 5 Hz (left), fs = 6 Hz (middle), and fs = 7 (right). The vibrating frequency of the string was fixed at 57 Hz.

cal to that measured with the accelerometer. When the voice ceased, the color signals disappeared immediately. The CDI vibratory artefact patterns became irregular when the SPL was too high, which might also cause the saturation artefact of Doppler color.

During sustained phonation, the vibratory movement of the mucosa generated the color artefact that extended vertically. Because both upper and lower margins of the VF were stationary, the horizontal width of the vibratory artefact should correspond to half of the mucosal wavelength (λ). Using the C^{++} image-processing software developed earlier (Shau et al. 1999), we measured the horizontal width (L_m) of the CDI color artefact under the VF for each US image (Fig. 8a) and took the average value typically over 5 to 7 sequential frames. Based on the model of finite string with fixed endpoints, the mean mucosal wavelength is simply given by $\lambda = 2\ L_m$. Therefore, we can use it to calculate the mean MWV (c) directly based on the F0 that is indicated by the spectrum analyzer, c = F0 λ. Figure 9a and b depicts the results of MWV measured for the men and women, respectively. In the sustained phonation in their comfortable pitch and soft intensity, the mean MWVs for the men vary from 2.1 to 10 m/s in a frequency range of 85 to 310 Hz; the women have MWVs that vary from 5.0 to 16.5 m/s in frequency range of 180 to 480 Hz. Women typically phonated at a higher F0, and the corresponding SPL was also higher. Therefore, the VF CDI vibratory artefacts for the women were much more irregular than that of the men due to higher SPL (as in Fig. 8b). The uncertainty in the MWV measurement was typically below 5% and the results were very repeatable.

Figure 10 shows the typical VF CDI for a woman patient with a polyp; the color artefacts are more irregular than that of normal phonation. With a hoarse voice, the motion of the VF with polyp caused asymmetrical artefacts as the mucosal waves propagated upward vertically. From the color codes, we found the subglottic mucosal wave with higher vibratory movement (on the right) was severely dampened as it moved across the polyp (to the left) and the "Africa" artefact pattern was altered.

Table 1. Effects of vibrating frequency (f) on the wavelength of CDI artefacts (λ_{CDI})

f (Hz)	c* (cm/s)	$\lambda^{\dagger}$ (cm)	λ_{CDI} (cm)	f/fs	$\lambda_{CDI} \cdot f/fs$ (cm)
57	406	7.13	0.417	9.5	3.97
119	492	4.14	0.198	19.8	3.93
161	550	3.42	0.146	26.8	3.92
190	591	3.11	0.126	31.7	3.99
204	610	2.99	0.115	34.0	3.91

Vibrating string phantom A: fs = 6 Hz.
* The TWV (c) were calculated based on the regression line (Fig. 6) from the data of photosensor measurements; $^{\dagger}\lambda$= traveling wave wavelength, $\lambda = c/f$.

Table 2. Effects of vibrating frequency (f) on the wavelength of CDI artefacts (λ_{CDI})

f (Hz)	c* (cm/s)	$\lambda^{\dagger}$ (cm)	λ_{CDI} (cm)	f/fs	$\lambda_{CDI} \cdot f/fs$ (cm)
16	938	58.6	1.50	2.7	4.00
28	938	33.5	0.87	4.7	4.05
36	938	26.0	0.66	6.0	3.94
54	938	17.4	0.45	9.0	4.06
83	938	11.3	0.29	13.8	3.99
178	1470	8.26	0.14	29.7	4.08
185	1470	7.95	0.13	30.8	4.04
192	1470	7.66	0.12	32.0	3.84
238	1470	6.18	0.10	39.7	4.16

Vibrating string phantom B; fs = 6 Hz.
* The TWVs (c) were measured with photosensors; $^{\dagger}\lambda = c/f$.

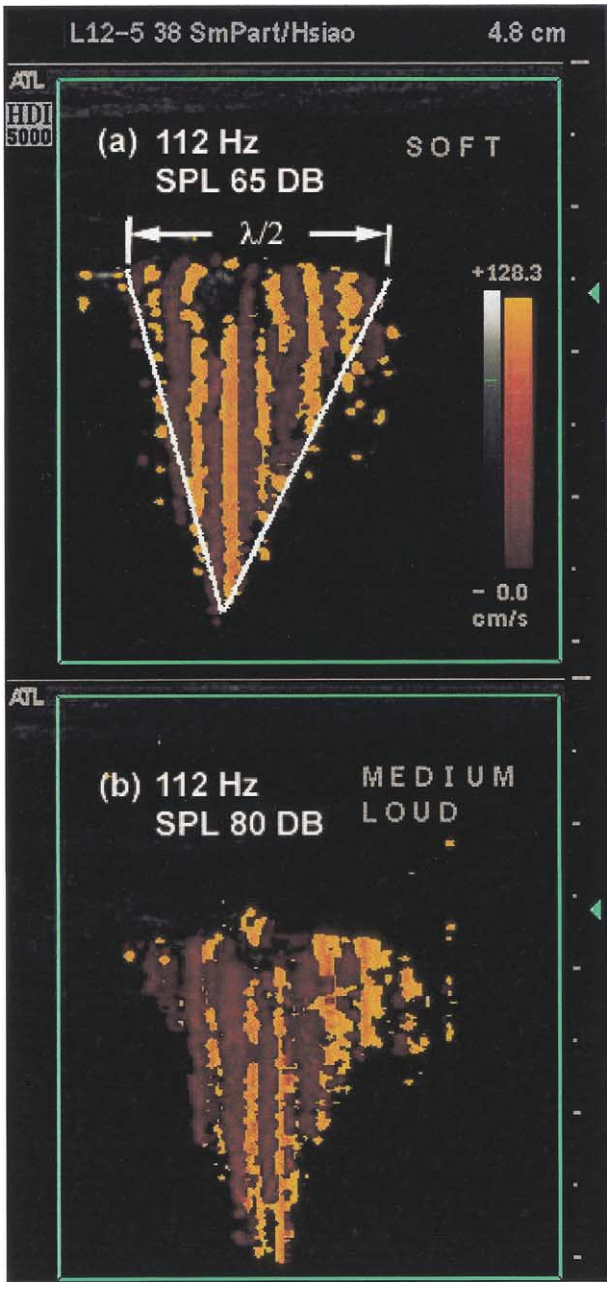

Fig. 8. Effects of sound pressure levels (SPL) on the CDI color artefacts for relatively the same phonation frequency f = 112 Hz. (a) SPL = 65 dB; (b) SPL = 80 dB. The width of the color artefact gives approximately the half wavelength of the mucosal wave, $L_m = \lambda/2$.

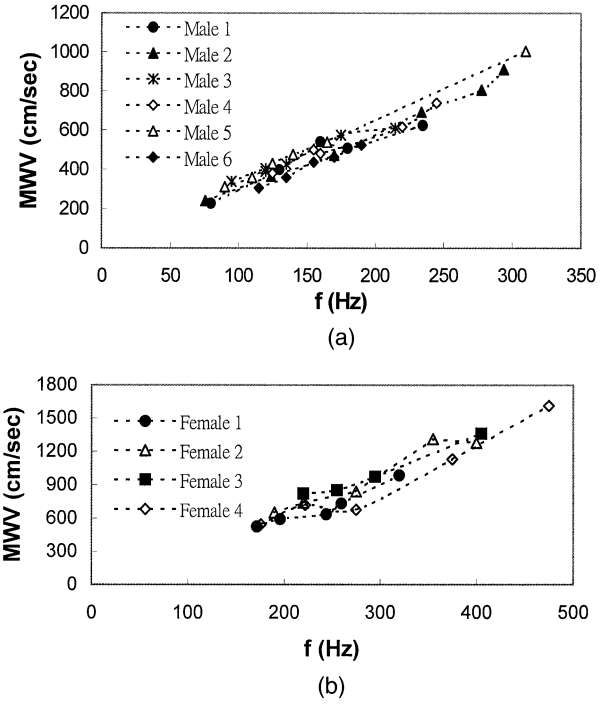

Fig. 9. Relationships between the vertical MWV and the fundamental frequency of the voice for (a) men (n = 6) and (b) women (n = 4) with normal phonation function.

DISCUSSION

Accurate quantitative assessment of the VF function is the goal that voice clinicians have long sought. To meet the requirements for routine laryngeal examination, the method must be easy to perform and analyze, cost-effective and with a minimum disturbance to the voice production. The medical US seems to be one of the best choices if the basic phenomena of sonography for the vibratory VF can be well understood.

CDI has been used extensively as a noninvasive tool for quantifying blood flows; however, little is known about its application on detecting high-frequency vibratory movements. Generally, medical US used clinically was inadequate to visualize the vibratory movement of the VF due to the limits in frame rate and spatial resolution. Although the A-M mode echoglottography may provide a better time-resolution, the complexity of the changes in VF shape during phonation creates very confusing echoes (Hertz et al. 1970; Holmer et al. 1973; Hamlet 1980; Miles 1989). Ooi et al. (1995) first used the CDI to identify vocal cord palsy based on the asymmetry of color flow patterns, but the CDI vibratory artefacts were somewhat misinterpreted.

The vibrating frequency, amplitude, the mass density and the acoustic impedance of the soft tissues were found to play important roles in the formation of US color artefacts. At a given CDI frame rate (f_s), the US system scanned through the region-of-interest (ROI) line-by-line sequentially; thus, for a finite string that vibrated at a frequency (f) higher than f_s, the string would appear in sinusoidal waveforms. The colored artefact strips were generated accordingly and the local color indicated the mean movement velocity and direction of

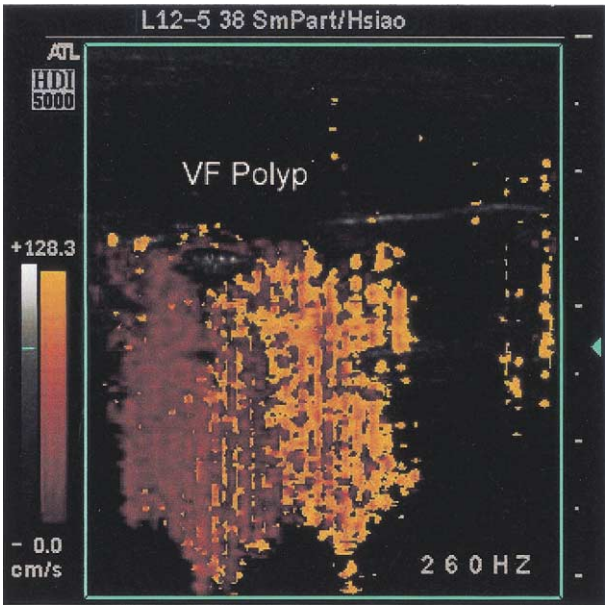

Fig. 10. VF CDI for a woman patient with a VF polyp. The mucosa vibrated at higher amplitude in subglottic area (on the right) and the movement was dampened as it moved across the polyp upward (to the left), which resulted in a hoarse voice.

the string at the time of Doppler sampling. Therefore, the wavelength of the color strips (λ_{CDI}) in CDI reflected the frequency of the vibratory motion relative to the US frame rate (f/f_s). The constant, 3.94, in eqn (4), was related to the equivalent line-scanning velocity (*i.e.*, 3.94 f_s cm/s) for the present CDI system setting.

As shown in Fig. 5a, we attached small plastic tapes on the surface of the rubber string to simulate the hardened spot on the VF; the strong color artefacts were observed to reflect from the sites of the tapes due to higher difference in acoustic impedance. For a small vibratory movement of uniform rubber string, the penetration depth of the color artefact was proportional to its velocity. It should be noted that the Doppler frequency aliasing might occur if the vibrating velocity exceeded the PRF Nyquist limit. The CDI frame rate may be responsible for the spatial aliasing; a lower PRF or Doppler velocity scale may result in frequency aliasing.

The CDI of the VF movement during sustained phonation exhibited similar color artefacts as that of the vibrating string (Fig. 4b, c), and the color artefacts were originated from the mucosal cover and air interface where acoustic discontinuity was encountered. In coronal view of the VF, the cover moved mediolaterally in the direction toward and away from the US transducer, and the color of the CDI artefacts represents the mean velocity of the vibrating mucosa. The vibrating frequency (f) predicted from the wavelength of color strips (λ_{CDI}) agrees with the F0 of both the voice recorded by microphone and the laryngeal vibration that was detected by accelerometer. Note that the vibratory movement of complex VF structure resulted in different HDVs along the mucosal surface vertically; however, the VF cover vibrated as a finite membrane with fixed ends because the artefact wavelengths (λ_{CDI}) along the mucosa were about the same. The width of the color artefacts in VF coronal view indicates the vertical extent that VF vibrates during phonation.

Although it has been well known that the "stiffness" of the VF greatly affects its vibratory movement in phonation, *in vivo* studies of human VF mechanical properties have been limited (Isshiki et al. 1985; Berke and Smith 1992). The measurements were invasive and were made during laryngeal surgery. Noninvasive measurements of human VF stiffness were focused on the propagation of mucosal wave observed from the oral side (Sercarz et al. 1992; Hanson et al. 1995). During voicing, the mucosal wave was observed to propagate upward from the mucosal upheaval (Yumoto et al. 1996).

Unlike the lateral length scale of the vocal cords that is identifiable with laryngostroboscopy, the vertical dimension of the VF during phonation cannot be seen easily because there is no natural landmark available. However, using CDI, the vertical length scale of the vibrating part of the mucosa can be visualized from the color artefacts (Fig. 8a), which leads to the mean MVW (c). As indicated in our *in vitro* study, the penetration depth of the color artefact was proportional to the movement velocity locally; thus, the "Africa" shape of the color artefact revealed the spanwise variation of MWV during the glottal cycle.

The mean MWVs for the men were found vary from 2.1 to 10 m/s in frequency range of 85 to 310 Hz at their comfortable pitch and SPL; these results agreed with those reported in the literature (Tran et al. 1993; Hanson et al. 1995). The women typically had higher MWV that varied from 5.0 to 16.5 m/s in a frequency range of 180 to 480 Hz. To our best knowledge, this is the first time that the effect of gender on the MWV has been reported because the edge of the mucosal wave is difficult to see by laryngostoboscopy in women (Hanson et al. 1995). With the increase in phonation frequency, the SPL for the voice was slightly raised because the threshold pressure increased with the F0 (Titze 1988). The women typically phonated at a SPL of about 5 to 10 dB higher than the men for the same vowel; their VF CDI vibratory artefacts were not as regular as those for the men phonating at a soft voice.

For the voice beyond a F0 of 350 Hz, the vibratory HDV of women would exceed the maximum Doppler velocity scale (128 cm/s) and the saturation color artefacts also appeared. The vibratory artefact may lose its uniformity in color strips when the SPL is high or satu-

rated; however, the width of the color artefact that gives the vertical extent of mucosal wave is not affected (Fig. 8a, b). Hirano (1974) studied the morphologic structure of the VF under different laryngeal adjustments; for a soft voice at low pitch levels both the VF cover and the body were very flexible and equally involved in the vibratory movement. For a loud voice at medium-high pitch level, the VF body increased its stiffness due to stronger contraction of vocalis muscle and the cover maintained its softness. The spotty CDI artefact that appears in high pitch and loud voice may be attributed to the vibratory interaction of the slackened VF cover and the stiff VF body.

Note that the VF stiffness would be different between the transverse and the longitudinal aspects. Comparisons of the changes of MWV for men and women VF showed the same trend with respect to the F0 (Fig. 9a, b). The women typically have shorter vocal cord lengths than the men (Kahane 1978; Titze 1989); therefore, their F0s of voice for a comfortable vowel are also higher. However, under normal phonation function, the mechanical properties of the VF cover for both men and women (based on the slope of their MWV vs. frequency) are about the same. All the MWV data fall into relatively the same curve and simply related to the phonation frequency.

The human MWV was slightly higher than that of canine (*i.e.*, 0.9 to 1.6 m/s, Sloan et al. 1993; 0.5 to 2.0 m/s, Titze et al. 1993; 0.76 to 2.2 m/s, Nasri et al. 1994) in the frequency range of 100 to 180 Hz. Although the infraglottic aspect of human VF vibrates in a similar manner as that of the canine, the intrinsic structures of their VF mucosa are very different (Yumoto et al. 1996). The cover of human VF was found to be thinner and stiffer than that of the canine, and the corresponding MWV was expected to be relatively higher.

This study represents the first attempt to measure the MWV *in vivo* using US. The characteristics of the mucosal wave are valuable clinically for evaluating vocal disorders. The CDI provided an insight into the dynamics of VF membranous structure during phonation. As demonstrated in the present study, the mucosal scars and mass lesions on the VF may result in abnormal TWV and different CDI vibratory artefacts. With the help of CDI artefacts, the VF location can be easily identified. It is feasible to apply the color artefacts to measure the MWV with a reasonable accuracy and quantify the human laryngeal function noninvasively using a commercially available US system. However, for the clinicians, the proper positioning of the US transducer in scanning the vibrating VF may take a little practice because the VF moves in a complex manner and changes its position during different pitches of phonation.

SUMMARY

In the effort to develop a noninvasive method for evaluating VF functions clinically, we identified the US CDI as a promising technique because it is simple, painless, with the least interference to the phonation path and no need for anesthesia. By tracing the color artefacts generated at the mucosa-air interface, the location of the VF can be easily found with US. The mechanism for the formation of vibratory color artefacts and their correlation with the vibrating tissues were demonstrated with string phantoms. The mean MWV was calculated based on the vibration of a finite string model with fixed ends, and the variation in MWV as it propagated vertically was revealed by the color and shape of the artefacts. The women subjects had shorter vocal cords than the men. Thus, their MWVs were found to extend from the men's data into a higher frequency range. The present method is versatile for the investigation of VF biomechanics in a broad range of frequency for different ages and genders. It is also applicable for the evaluation of phonation function for vocal disorders that alter the vibratory movement of the mucosa. The use of CDI artefacts may extend the laryngeal US into a bright future in routine clinical service.

Acknowledgement—This research was supported by Grant NSC 89-2320-B-002-149 M08.

REFERENCES

Achenbach JD. Wave propagation in elastic solids. Evanston, IL: Elsevier Scientific, 1984:30–33.

Baken RJ, Orlinkoff RF. Clinical measurement of speech and voice, 2nd ed. San Diego, CA: Singular Publishing, 2000:393–451.

Berke GS. Intraoperative measurement of the elastic modulus of the vocal fold. Part 1. Device development. Laryngoscope 1992;102: 760–769.

Berke GS, Smith ME. Intraoperative measurement of the elastic modulus of the vocal fold. Part 2. Preliminary results. Laryngoscope 1992;102:770–778.

Fetter AL, Walecka JD. Theoretical mechanics of particles and continua. Singapore: McGraw-Hill, 1980:207–263.

Friedman EM. Role of ultrasound in the assessment of vocal cord function in infants and children. Ann Otol Rhinol Laryngol 1997; 106:199–209.

Garel C, Legrand I, Elmaleh M, Contencin P, Hassan M. Laryngeal ultrasonography in infants and children: Anatomical correlation with fetal preparations. Pediat Radiol 1990;20:241–244.

Hanson DG, Jiang J, D'Agostino M, Herzon G. Clinical measurement of mucosal wave velocity using simultaneous photoglottography and laryngostroboscopy. Ann Otol Rhinol Laryngol 1995;104:340–349.

Hamlet SL. Ultrasonic measurement of larynx height and vocal fold vibratory pattern. J Acoust Soc Am 1980;68:121–126.

Hertz CH, Lindstrom K, Sonesson B. Ultrasonic recording of the vibrating vocal folds. Acta Otolaryngol 1970;69:223–230.

Hirano M. Morphological structure of the vocal cord as a vibrator and its variations. Folia Phoniatr 1974;26:89–94.

Hirano M. Clinical examination of voice. Wien-New York: Springer-Verlag, 1981.

Holmer NG, Kitzing P, Lindstrom K. Echoglottography. Acta Otolaryngol 1973;75:454–463.

Hsiao TY, Wang CL, Chen CN, Hsieh FJ, Shau YW. Noninvasive

assessment of laryngeal phonation function using color Doppler ultrasound imaging. Ultrasound Med Biol 2001;27:1035–1040.
Ishizaka K, Matsudaira M. Synthesis of voiced sound from a two-mass model of the vocal cords. Bell Syst Tech J 1972;51:1233–1268.
Isshiki N. Phonosurgery. Theory and practice. Tokyo: Springer-Verlag, 1989.
Isshiki N, Ohkawa M, Goto M. Stiffness of the vocal cord in dysphonia—its assessment and treament. Acta Otolaryngol (Stockh) 1985; Suppl.419:167–174.
Kahane J. A morphological study of the human prepubertal and pubertal larynx. Am J Anat 1978;151:11–20.
Lin E, Jiang J, Hone S, Hanson DG. Photoglottographic measures in Parkinson's disease. J Voice 1999;13:25–35.
Miles KA. Ultrasound demonstration of vocal cord movements. Br J Radiol 1989;62:871–872.
Nasri S, Sercarz JA, Berke GS. Noninvasive measurement of traveling wave velocity in the canine larynx. Ann Otol Rhinol Laryngol 1994;103:758–766.
Ooi LL, Chan HS, Soo KC. Color Doppler imaging for vocal cord palsy. Head Neck 1995;17:20–23.
Raghavendra BN, Horii SC, Reede DL, et al. Sonographic anatomy of the larynx, with particular reference to the vocal cords. J Ultrasound Med 1987;6:225–230.
Sasaki CT, Weaver EM. Physiology of the larynx. Am J Med 1997; 103:9s–18s.
Sawashima M. Fibreroptic observation of the larynx and other speech organs. In: Sawashima M, Cooper FS, eds. Dynamic aspects of speech production. Tokyo: University of Tokyo Press, 1977:31–46.
Schindler O, Gonella ML, Pisani R. Doppler ultrasound examination of the vibration speed of vocal folds. Folia Phoniatr 1990;42:265–272.
Sercarz JA, Berke GS, Ming Y, Gerratt BR, Natividad M. Videistroboscopy of human vocal fold paralysis. Ann Otol Rhinol Laryngol 1992;101:567–577.
Shau YW, Wang CL, Shieh JY, Hsu TC. Noninvasive assessment of the viscoelasticity of peripheral arteries. Ultrasound Med Biol 1999;25:1377–1388.
Sloan SH, Berke GS, Garratt BR, Kreiman J, Ye M. Determination of vocal fold mucosal wave velocity in an *in vivo* canine model. Laryngoscope 1993;103:947–953.
Tanaka S, Hirano M. Fiberscopic estimation of vocal fold stiffness *in vivo* using the sucking method. Arch Otolaryngol Head Neck Surg 1990;116:721–724.
Titze IR. The physics of small-amplitude oscillation of the vocal folds. J Acoust Soc Am 1988;83:1536–1552.
Titze IR. Physiological and acoustic differences between male and female voices. J Acoust Soc Am 1989;85:1699–1707.
Titze IR, Jiang JJ, Hsiao TY. Measurement of mucosal wave propagation and vertical phase difference in vocal fold vibration. Ann Otol Rhinol Laryngol 1993;102:58–63.
Tran QT, Berke GS, Gerratt BR, Kreiman J. Measurement of Young's modulus in the *in vivo* human vocal folds. Ann Otol Rhinol Laryngol 1993;102:584–591.
Yumoto E, Yoshimi K, Toshihiro M. Vocal fold vibration viewed from the tracheal side in living human beings. Otolaryngol Head Neck Surg 1996;115:329–324.